Title
Bmi1+ Progenitor Cell Dynamics in Murine Cornea During Homeostasis and Wound Healing

Journal
Stem Cells, 36(4)

ISSN
1066-5099

Authors
Kalha, Solja
Shrestha, Bideep
Navarro, Maria Sanz
et al.

Publication Date
2018-04-01

DOI
10.1002/stem.2767

Peer reviewed

HHS Public Access

Author manuscript

Stem Cells. Author manuscript; available in PMC 2019 April 01.

Published in final edited form as:

Stem Cells. 2018 April ; 36(4): 562–573. doi:10.1002/stem.2767.

Bmi1+ progenitor cell dynamics in murine cornea during homeostasis and wound healing

Solja Kalha[a], **Bideep Shrestha**[a], **Maria Sanz Navarro**[a], **Kyle B. Jones**[b], **Ophir D. Klein**[b,c], and **Frederic Michon**[a,*]

[a]Helsinki Institute of Life Science, Institute of Biotechnology, University of Helsinki, 00014, Helsinki, Finland [b]Department of Orofacial Sciences and Program in Craniofacial Biology, UCSF, San Francisco, USA [c]Department of Pediatrics and Institute for Human Genetics, University of California San Francisco, San Francisco, CA 94143, USA

Abstract

The outermost layer of the eye, the cornea, is renewed continuously throughout life. Stem cells of the corneal epithelium reside in the limbus at the corneal periphery and ensure homeostasis of the central epithelium. However, in young mice, homeostasis relies on cells located in the basal layer of the central corneal epithelium. Here, we first studied corneal growth during the transition from newborn to adult and assessed Keratin 19 (*Krt19*) expression as a hallmark of corneal maturation. Next, we set out to identify a novel marker of murine corneal epithelial progenitor cells before, during and after maturation, and we found that *Bmi1* is expressed in the basal epithelium of the central cornea and limbus. Furthermore, we demonstrated that *Bmi1+* cells participated in tissue replenishment in the central cornea. These *Bmi1+* cells did not maintain homeostasis of the cornea for more than three months, reflecting their status as progenitor rather than stem cells. Finally, after injury, *Bmi1+* cells fueled homeostatic maintenance, whereas wound closure occurred via epithelial reorganization.

Graphical abstract

*Corresponding author: Frederic Michon, Ph.D., Helsinki Institute of Life Science, Institute of Biotechnology, University of Helsinki, Viikinkaari 5 00790 Helsinki, Finland. frederic.michon@helsinki.fi.

Author contributions:

Solja Kalha: conception and design, collection and assembly of data, data analysis and interpretation, manuscript writing

Bideep Shrestha: collection and assembly of data

Maria Sanz Navarro: collection and assembly of data

Kyle Jones: collection of data, conception and design

Ophir Klein: conception and design, manuscript writing, final approval of manuscript

Frederic Michon: conception and design, data analysis and interpretation, manuscript writing, final approval of manuscript

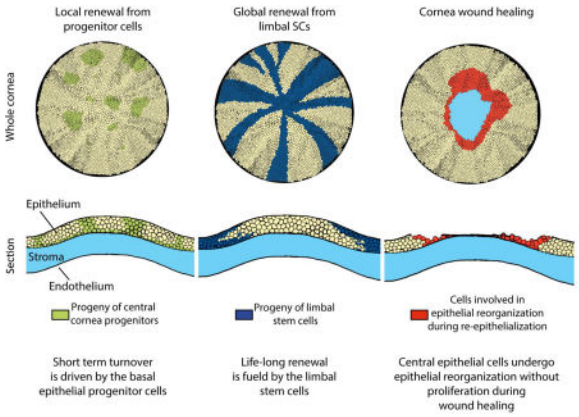

Keywords

cornea; Bmi1; stem cell; progenitor; maturation; renewal; wound healing

Introduction

The cornea is the transparent layer that covers the surface of the eye. It serves as a barrier to pathogens and water loss, and it forms a refractive layer essential for vision. The outermost layer is formed by the corneal epithelium, where cells are strictly adherent to each other and in contact with the physical environment. Basal epithelial cells sit on the basement membrane, and suprabasal and superficial epithelial cells make up the following 3–4 epithelial cell layers. The superficial layer faces the tear film, a source of hydration and nutrients to the epithelium.

Corneal epithelium is renewed throughout life. Stem cells that fuel this renewal are situated at the periphery of the cornea, in a ring-like structure called the limbus [1]. Early work identified label retaining cells (LRCs) of the cornea in the limbus, suggesting that the limbus is a stem cell niche (SCN) which houses the limbal stem cells (LSCs) [2,3]. Several studies have shown centripetal renewal of the corneal epithelium from the limbus to the central cornea using genetic fate mapping [4–7]. However, renewal patterns exhibit temporal and species-specific differences [8]. Collinson et al. showed that in young mice, the central corneal cells maintain the epithelium, and limbal renewal only begins at about 5 weeks of age [4]. Genetic fate mapping showed that central corneal renewal is a temporary phenomenon. By 10–14 weeks of age, the central cornea clones are replaced by progeny originating from the limbus and reaching the center of the cornea. This centripetal renewal pattern forms clonal stripes elongating from the limbus to the central cornea [4,5,9]. The progressive appearance of limbal-based renewal defines the end of murine corneal maturation.

Murine eyelid opening occurs at around postnatal day (P) 14, concomitantly with the beginning of epithelial stratification [10], which is complete by P21 [10]. Eyelid opening and epithelial stratification are followed by changes in the molecular identity of the corneal epithelial cells. *α9β1 integrin* is expressed in the entire murine cornea at birth, but is lost

from the central cornea at P14 [11]. The expression domain regresses progressively to the peripheral cornea and is fully established in the limbus by 6 weeks of age, at the same time as limbal renewal begins. In human embryos, *Keratin 14* (*Krt14*) is first expressed in the entire cornea, but it becomes restricted to the limbus before birth [12]. In mouse, *Krt14* expression decreases in the upper epithelial layers and is limited to the basal cells of the central cornea at P10 [13]. By 10 weeks of age, the *Krt14+* stem and progenitor cells are located in the murine limbus [9]. Markedly later, by 12 weeks of age, central corneal epithelial cells express *Keratin 12* (*Krt12)*, which is proposed to be a terminal differentiation marker [13]. The limbal location of undifferentiated epithelial cells is supported by the lack of *Krt12* expression [1]. Molecular maturation of the cornea shows that undifferentiated cells are located in the limbus. However, exactly how and from which cells the SCN is established remains elusive.

Several groups have proposed markers for epithelial stem cells in adult cornea. The expression of *Bmi1*, a polycomb ring finger protein, has been reported in stem cells in a number of other organs [14–17]. Furthermore, *Bmi1* expression was detected in the human limbus [18]. *Bmi1* expression was later confirmed in an *in vitro* model of naïve human limbal epithelial cells and limbal holoclones from pig [19,20]. In other organs, including the bone marrow, central and peripheral nervous systems and tooth, *Bmi1* functions in stem cell self-renewal [14–16]. The absence of *Bmi1* results in severe defects in skeletal patterning, intestinal development and hematopoiesis [15,21,22], likely as a result of oxidative damage in $Bmi1^{-/-}$ cells [23]. Thus, the identification of *Bmi1* expression in the cornea opens a door into studying tissue renewal of the corneal epithelium.

As the ocular surface is an exposed tissue, it is regularly challenged by physical damage. Previously, wound healing studies have been combined with genetic fate mapping of epithelial cells, using *Krt14* as a driver for reporter expression and employing a chemical wound [6]. In this study, the limbal contribution during wound healing increased with the severity of the wound, whereas mild wounds did not require limbal input for healing. Furthermore, Majo et al., challenged the concept of limbal renewal and showed that the central cornea houses cells that are able to repopulate the ocular surface upon injury [20]. However, genetic fate mapping from a defined stem cell population in homeostasis and injury has not been performed, making it difficult to dissect the identity of these cells. In light of differing renewal patterns in young and mature mice, it is important to consider the age of the mouse during renewal, injury and maintenance of homeostasis.

In this study, we investigated corneal maturation in detail and characterized *Krt19* in the maturation process. Furthermore, we identified the expression of *Bmi1* in murine corneal epithelium and used this marker to study cornea renewal. We found that *Bmi1+* cells localized to the basal epithelium in the central cornea and limbus. Interestingly, genetic fate mapping demonstrated that a subset of *Bmi1+* cells behaved as progenitors. These cells renewed the corneal epithelium locally and were replaced after 4–8 weeks. Moreover, they were not involved in wound healing after ocular surface injury. Taken together, these observations demonstrate that the central cornea harbors cells that act as progenitors but have a limited life span.

Materials and methods

Animals

Unless otherwise indicated, we used outbred NMRI mice in our experiments. For the label retaining experiment, we used outbred ICR mice. The generation and characterization of *Bmi1*^{CreERT} and *R26R*^{LacZ} mice have been described earlier [24,25]. Both lines were maintained in outbred NMRI background, but crossed with each other to obtain *Bmi1*$^{CreERT/wt}$;*R26R*$^{LacZ/wt}$ animals for genetic inducible fate mapping. Vaginal plug day was counted as embryonic day (E) 0.5. Postnatal days are numbered from the date of birth (P0). All animal experiments were approved by the national Animal Experiment Board.

Histology and immunostaining

Mouse tissues (eyeballs or whole heads) were fixed in 4 % PFA (paraformaldehyde), dehydrated, and embedded in paraffin. E18.5 head samples were decalcified with 0.5 M EDTA (ethylenediaminetetra acetic acid) for two weeks before paraffin embedding. 5μm-thick paraffin sections were stained with hematoxylin (Sigma-Aldrich) and eosin (Sigma-Aldrich). For immunofluorescence, sections were pretreated for clearing and rehydration, followed by antigen retrieval for two hours in a pressure cooker (Retriever 2100, Aptum Biologics), immersed in 10 mM sodium citrate buffer. Retrieval was followed by preblocking with 3 % hydrogen peroxide (Sigma-Aldrich) in methanol (Sigma-Aldrich) and tissue permeabilization with 0.3 % Triton-X in PBS. After antigen blocking with 10 % serum in 1 % BSA (bovine serum albumin) in PBS, sections were incubated overnight with a primary antibody in the blocking solution. We used antibodies for Keratin 19 (Abcam, ab52625) and β-catenin (BD Biosciences, 610154) in 1:100 and Ki67 (Abcam, ab16667) and Bmi1 (Abcam, ab38295) in 1:200 concentrations, followed by incubation with Alexa 488 or 568 -conjugated secondary antibodies (Thermo Scientific, A11008 or A10042) and Hoechst (Thermo Scientific) for counterstaining. For immunostaining on Bmi1 (Cell Signaling, 6964S), we used abovementioned pretreatments, followed by preblocking; 1 % hydrogen peroxide in methanol and tissue permeabilization as above. Samples were blocked using 3 % BSA, 20 mM $MgCl_2$, 0.3 % Tween-20 (Sigma-Aldrich) and 5 % FBS (fetal bovine serum) (Hyclone, GE Healthcare) in PBS. Primary antibody was incubated overnight in 1:200 concentration in the blocking solution and subsequently in an anti-rabbit HRP-conjugated secondary antibody (ImmunoLogic). We performed a 3,3-diaminobenzidine staining (Vector Laboratories) and used 50% Gills Hematoxylin (Sigma-Aldrich) for counterstaining.

Eye size measurements and quantification of *Ki67+* corneal epithelial cells

Eye sizes were measured from fresh, enucleated eyes (n=3–7/time point). Measurements were done using the ZEN software (blue edition, 2009–2011, 1.0.0.0., Carl Zeiss). Growth categories were based on statistical difference between age pairs as follows: intense ($p \leq 0.05$ between adjacent age pairs), moderate ($p \leq 0.05$ between non-adjacent age pairs) or no growth (size differences between ages did not differ statistically). *Ki67+* cells were counted manually after immunofluorescence on 20 serial sections (5 μm intervals) from 3 different individuals. Each corneal epithelium was divided into two limbal, two peripheral and one central compartment that encompass 6.4 % (2x), 14.6 % (2x) and 58 % of the epithelium,

respectively (Supporting Information Fig. S1A), using the ZEN software (blue edition, 2009–2011, 1.0.0.0., Carl Zeiss). *Ki67+* cells were calculated separately for each compartment and then normalized to the area (A) of the compartment by using the formula *Ki67+* cells/(Ax5x20). Coverage of the cornea was calculated with $\pi \times ((\sqrt{cornea\ r}) + (\sqrt{cornea\ height}))/4 \times \pi \times (\sqrt{eyer})$.

In situ RNA hybridization

In situ RNA hybridization was performed using RNAscope technology (Advanced Cell Diagnostics), following a manufacturer's protocol. We used a mouse *Bmi1* probe (target region 3096 – 3549 of NM_007552.4) and a colorimetric revelation kit (Advanced Cells Diagnostics). Sections were photographed using an Olympus AX70 microscope.

Genetic inducible fate mapping

For genetic fate mapping of *Bmi1+* cells in embryonic stages, pregnant females were injected (i.p.) twice with tamoxifen (Sigma-Aldrich). At P4 and P5, mice were injected (i.p.) twice with tamoxifen (Sigma-Aldrich) and from the age of 4 weeks onwards, tamoxifen was administrated orally (i.g.) on two consecutive days. We prepared tamoxifen at 50mg/ml in corn oil (Sigma-Aldrich) and gave it at the daily dose of 10mg/30 g at all stages. For each time point, we sacrificed three experimental animals. X-Gal staining was performed as previously described [26] and sections were counterstained with Nuclear FAST red (Fluka) supplemented with thymol (Sigma-Aldrich). Sections were photographed with an Olympus AX70 microscope.

Labeling and detecting label retaining cells

We gave a single injection of 5-bromo-2'-deoxyuridine (BrdU, GE Healthcare) at 0.6 mg/animal to label cycling cells. BrdU staining followed the abovementioned immunofluorescent staining protocol, excluding methanol blocking. We used anti-BrdU antibody in 1:400 (GE Healthcare, RPN202).

Cornea injury

We used 4 week old mice (three littermates per time point) for the initial cornea injury model. Injuries were performed under anesthesia. To induce anesthesia, we gave the experimental animals a mixture of ketamine and medetomidine, 75 mg/kg + 1 mg/kg (i.p.) (Orion Pharma, Intervet). Then, we scraped away a circular area of the central cornea with Algerbrush 2, BR2-5 0.5 mm (Alger Company) ocular burr. We took care not to injure peripheral and limbal regions. Subsequently, we stained the ocular surface with 0.1 % fluorescein (Sigma-Aldrich) and photographed it under cobalt blue light with a Nikon SLR camera. Then, we proceeded to either euthanasia (0 h time point) or waking the animals up with a pulse (18 and 72 h time points). As a pulse, we used atipamezol 0.5 mg/kg (i.p.) (Orion Pharma). For analgesics, we administered buprenorphine, 0.05–0.1 mg/kg, (i.p.) (Invidior). If not sacrificed immediately after wounding, we gave the experimental animals carprofen, 5 mg/kg (i.p.) (Norbrook) and eye ointment (Dechra) daily until the end of the experiment. We did not find infection or inflammation in any animal. In addition, we used $Bmi1^{CreERT/wt};R26R^{LacZ/wt}$ animals for an experiment where cornea injury was combined

with genetic fate mapping. Cre activation was induced as described above at the age of 6 weeks. We performed the injury two weeks later, as described in this section. Eyes were enucleated and processed for X-gal staining and then imaged with Zeiss Lumar stereomicroscope. The right eye of each animal was not scraped in neither case and thus served as a control. We estimated the epithelial thickness after wounding from hematoxylin and eosin stained sections. Thickness was measured from 4–6 wounded and 4–6 bilateral, unwounded eye sections using the ZEN software (blue edition, 2009–2011, 1.0.0.0., Carl Zeiss). We took measurements from two different zones, the exposed region and the peripheral cornea. The exposed region was the area in the center of the cornea that was scraped at 0 hour and in the center of the cornea. Peripheral cornea measurements were taken 400 μm from the limbus, where the epithelium was intact.

Statistics

Eye and cornea size measurements, *Ki67+* cell quantification and epithelial thickness after injury were tested statistically for ANOVA (analysis of variance), combined with Tukey or Bonferroni post hoc tests and, when needed, with Kruskal-Wallis test with pairwise comparisons. We used $p \leq 0.05$ as significance threshold.

Results

Keratin 19 expression pattern shows early murine limbal maturation

The renewal pattern of murine corneal epithelium was suggested to be dependent on the degree of maturation. Expression patterns of *Krt14* and *Krt12* were previously used as markers to evaluate this maturation [9,13]. However, these markers do not highlight the timing of establishment of the limbal SCN, as neither is exclusively expressed by the LSCs. Therefore, to evaluate the chronological events that lead to the formation of the niche, we studied *Keratin 19* (*Krt19*) expression in the postnatal cornea. Interestingly, *Keratin 19* (*Krt19*) expression was previously detected in the basal epithelium of adult human and murine limbus and human conjunctiva [27–31]. We followed *Krt19* expression from E13.5 to P21. We detected *Krt19* throughout the embryonic corneal epithelium from E13.5 to E18.5 (data not shown), but the postnatal expression pattern changed progressively (Fig. 1A). Immediately after birth, *Krt19* was homogeneously detected in the epithelium. By P7, the basal epithelium was devoid of *Krt19+* cells in the central cornea. After P7, when corneal epithelial stratification begins, *Krt19* expression gradually decreased from the central and peripheral cornea, until it was totally lost by P21. Thereafter, the *Krt19* expression pattern was similar to adult cornea. Similarly, the *Krt8* expression domain changed from central cornea to limbus in parallel to changes in expression of *Krt19* (Supporting Information Fig. S2). In contrast to *Krt12* and *Krt14* expression, our results demonstrated the swift loss of *Krt8* and *Krt19* expression in the central cornea.

To understand if the process of corneal maturation was concomitant with a change in the eye morphology, we analyzed the growth of the mouse eyeball and cornea. We classified the growth patterns into three categories: intense, moderate or no growth. The most intense period of growth occurred during the first postnatal week, and then the eyeball grew steadily until 4 weeks of age, when the eyeball reached its adult size (Fig. 1B). Interestingly, the

mouse cornea growth pace was distinct from that of the eyeball. The cornea underwent two waves of intense growth. The first one was concurrent with the intense growth period of the eyeball during the first week after birth. The second period of intense growth was after the opening of the eyelid and the stratification of the cornea, between P21 and 4 weeks of age (Fig. 1C). Both waves were followed by a period of moderate growth (Fig. 1C). The cornea reached adult size by 16 weeks of age (Fig. 1C), long after the eyeball had stopped growing. Additionally, our measurements showed that the area covered by the cornea expanded as well. At birth, the mouse cornea covered 18% of the eyeball. By one year of age, the coverage increased up to 37%.

To investigate the input of proliferating cells to cornea growth, we quantified *Ki67+* cells in the mouse corneal epithelium from P0 to 24 weeks of age (Fig 1D). *Ki67+* cells were detected in the limbus, peripheral cornea and central cornea at all ages (Supporting Information Fig. S1B). The proportion of *Ki67+* cells was maintained at a steady level relative to the size of the cornea, increasing as the cornea grew larger (Fig. 1D). Our observations showed a constant rate of cell proliferation, sustaining first the cornea growth, then stratification, and finally constant renewal. Collectively, these results, combined with the *Krt8* and *Krt19* expression pattern, reflected the timeline and events of murine corneal maturation, and the early establishment of adult renewal framework. Therefore, we used 4 and 24 week old animals to study further cornea epithelial renewal.

Bmi1 expression is found early in the developing murine cornea

Previous studies had shown that the expression of *Bmi1* followed that of known limbal markers, *p63* and Keratin 15 (*Krt15*), in adult human cornea [18,32]. Notably, *p63* and *Krt15* become restricted to human limbus already before birth [32]. Therefore, we investigated *Bmi1* expression and the fate of *Bmi1+* cells during mouse cornea morphogenesis. We detected prominent expression of *Bmi1* from E12.5 until E18.5 throughout the corneal epithelium (Supporting Information Fig. S3). As *Bmi1* expression was previously reported to be restricted to the limbus in adult human cornea [18], we investigated if the postnatal timing of cornea maturation in mice had an influence on *Bmi1* expression pattern. We observed *Bmi1* expression in the basal and suprabasal epithelial layers before epithelial stratification (Fig. 2). After epithelial stratification at P14, *Bmi1* was present in all layers, however, a few cells were *Bmi1* negative. We performed an inducible genetic fate mapping experiment starting from P4 and observed the generation of epithelial clones from *Bmi1+* cells after two weeks or longer of chase (Supporting Information Fig. S4). Concomitant signal activation in the retina confirmed that a chase of two weeks is necessary for the *Bmi1+* progeny to be visible. Thus, *Bmi1+* cells participated actively in cornea growth during maturation.

Bmi1 is expressed in corneal epithelial progenitor cells

As the expression of *Bmi1* seemed broader than expected from a stem cell population, we investigated *Bmi1+* cells in the maturing and fully matured murine cornea. We used immunostaining and highly sensitive RNA *in situ* hybridization (RNAscope) to visualize subtle changes in *Bmi1* expression. Unexpectedly, we did not detect any change of *Bmi1* protein or RNA expression pattern over time (Fig. 3). Almost all basal epithelial cells were

Bmi1+, while few suprabasal cells expressed *Bmi1*. Notably, we detected some *Bmi1*-negative cells scattered in the basal layer of the central cornea.

Next, we analyzed participation of *Bmi1+* cells in cornea renewal. Inducible genetic fate mapping revealed a remarkable pattern of corneal renewal (Fig. 4). First, we studied the progeny of labeled cells using the $Bmi1^{CreERT/wt};R26R^{LacZ/wt}$ mouse model in 4-week-old animals, which have a recently matured cornea. The *Bmi1+* cell progeny arose in clusters, displaying a patchy pattern in central, peripheral and limbal cornea two weeks after induction (Fig. 4B). The cluster remained until 4 weeks of chase, but disappeared at 8 weeks. However, rare progeny stripes from the peripheral cornea formed at 8 weeks and were present until 16 weeks of chase (Fig. 4C). By 20 weeks of chase, we no longer detected the progeny of the originally labelled *Bmi1+* cells (Fig. 4B). Long-term follow up of corneal renewal did not show persistent or new generation of epithelial cells from the originally labelled *Bmi1+* cells. Histological analysis showed that the described clusters arose from *Cre+* cells (Fig. 4D) and *Bmi1+* clones grew larger with longer time intervals and expanded centripetally as well, also in the basal layer. Then, to understand if these observations were age-dependent, we applied the same approach to older animals. We conducted a similar fate mapping experiment with 24-week-old mice (Fig. 5A). In this experiment, we observed rare, small, *Bmi1+* cell clusters after 2–8 weeks of chase (Fig. 5B). These clusters disappeared upon longer chase times.

Even though *Bmi1* is expressed throughout the basal layer, X-gal does not stain a homogeneous area throughout the cornea. This could be due to low recombination efficiency or stochastic silencing due to variegation of transgene expression [33]. Regardless, our results are in line with the previous report on mouse cornea, such that the epithelial renewal decreases upon aging [5,34]. The progressive loss of *Bmi1+* cell progeny in fate mapping led us to assess the distribution of *Ki67+* cells and LRCs in the cornea. Our results clearly indicated that the *Bmi1+* population also contains the proliferative cells of the central cornea (Supporting Information Fig. 5A). In addition, we used BrdU incorporation to visualize the proliferative cells in central cornea and limbus (Supporting Information Fig. 5B-C). Taken together, our observations reflected the temporary maintenance of the central cornea epithelium by progenitor cells located in the basal cell layer, irrespective of the age of the animal.

Bmi1+ cells do not proliferate during wound healing

As our results pointed to the involvement of Bmi1+ cells in local renewal, we decided to test the impact of these progenitors on corneal wound-healing. Therefore, we performed an injury repair assay, using an *in vivo* epithelial scraping wound. This procedure removes only a selected region of the epithelium, leaving the rest of the epithelium unaffected. Importantly, we did not observe corneal opacification, neovascularization or conjunctivalization during or after healing (data not shown).

Repair after injury differs from homeostatic renewal in many organs. We assayed the role of *Bmi1+* progenitor cells in corneal wound healing after scraping the epithelium. *Bmi1* reporter expression was induced at 6 weeks of age (Fig. 6A), just after cornea maturation was finished. As described above, we observed *Bmi1+* cell clusters in the central cornea,

excluding the scraped region, immediately after wounding (Fig. 6B). An epithelial wound was still visible 18 hours after injury, but genetic fate mapping of *Bmi1+* cells did not reveal a pattern that differed from homeostasis. By 72 hours, the epithelial wound had closed fully. This was confirmed by genetic fate mapping; cell clusters appeared in central, peripheral and limbal cornea, suggesting a full closure of the wound, followed by a restoration of normal renewal (Fig. 6B). Interestingly, we did not observe any changes in the *Bmi1+* cell progeny patterning. In addition, we performed a similar epithelial wounding experiment without the inducible genetic fate mapping (Supporting Information Fig. S6A). In line with Fig. 6, this assay indicated that injury did not induce accelerated cell proliferation (Supporting Information Fig. S6B). In search of possible alternative wound healing mechanisms, we studied the morphology of the epithelium in the proximity and at a distance from the wound. 18 hours after injury, the epithelium was markedly thinner (Fig. 7A). This region only contained the basal and first suprabasal cells but lacked the superficial cells (Fig. 7C). However, 72 hours after wounding, the cornea had healed (Fig. 7C). The thickness of the epithelium remained unchanged in the peripheral cornea during wound healing (Fig. 7B). These observations pointed towards a drastic epithelial reorganization that ensured a swift re-epithelialization to heal the cornea after epithelial scraping.

Discussion

The mouse cornea provides a tractable system to study epithelial stem cells. Several groups have shown that the corneal stem cells reside in the limbus [4–7]. It was proposed that postnatal corneal epithelium renews itself locally, apparently without limbal input, until approximately 5 weeks of age [4,5]. After that, renewal from LSCs is activated [4,5]. In this study, we focused on the corneal maturation and renewal pattern from birth to adulthood, and we found that regardless of the age of the animal, the murine corneal epithelium is renewed locally by progenitors expressing *Bmi1*. Importantly, limbal-based renewal replaces these progenitors every 4 to 8 weeks.

Like several other mammals, the mouse has closed eyelids at the time of birth, and eyelid opening happens at about P14 [10]. We observed that the eye grows continuously until 8 weeks of age, as previously reported [35]. Unlike in the human cornea, where proliferative cells shift from central cornea to limbus during a gestational maturation [26], we did not detect a similar change in the distribution of *Ki67+* cells during the maturation process in mouse. Our analysis showed that cornea growth was coupled to a steady level of *Ki67+* cells, relative to volume, at all ages.

Previous reports on murine cornea have shown a late timeline for corneal maturation at the molecular level. The mature and differentiated *Krt12+* corneal epithelial cells were observed in the central corneal epithelium by 12 weeks of age [13]. Strikingly, the chronology of LSN establishment, via *Krt19* and *Krt8* expression pattern, is much shorter. This differential timeline would indicate that the limbal territory is already set by P21, and that the populations labelled by these keratins mature faster than the *Krt12+* population. Interestingly, the chronology we observed with *Krt19* and *Krt8* expression is similar to the timeline of *α9β1 integrin+* domain establishment, reported earlier [11]. Importantly, the *Krt19+* cells locate to the superficial cell layer of the limbus. Therefore, our results suggest

that the limbal SCN is established early during murine cornea maturation. This niche contains a superficial layer that expresses *Krt19* and which we propose provides support that is necessary for maintenance of the SCN. Consequently, epithelial renewal originating from the limbus could start as early as 4 weeks of age.

Genetic fate mapping provides a powerful tool to study tissue renewal. To date, no marker other than *Krt14* has been used to genetically fate map a restricted corneal cell population [6,7]. While *Bmi1* expression in human was reported to be restricted to the limbus [18], the basal cell layer of the central mouse cornea contains mainly *Bmi1+* cells already early on during cornea morphogenesis. Our genetic fate mapping and label retaining experiments show that a subset of *Bmi1+* cells locally renew the corneal epithelium in a temporary fashion. We propose that a sub-population of the *Bmi1+* cells are progenitor cells that will be replaced by limbal renewal. We found that *Bmi1+* cell clusters maintained the corneal epithelium for 4–8 weeks after induction. This period thus reflects the maximum length of central corneal turnover time that is driven by the basal *Bmi1+* cells. This observation shows that local renewal occurs over a longer period than was postulated in an earlier study, where progenitor cells exhibited a faster turnover rate [3]. Indeed, our data are in line with a more recent observation, where central corneal patches were detectable even 8–10 weeks after induction of a ubiquitous reporter [5]. After the loss of proliferative potential of the epithelial progenitor cells, new cells are produced by LSCs [3]. Thus, these two compartments are dynamically coupled to maintain tissue homeostasis.

When we analyzed 24-week-old animals with fate mapping, we saw a lower incidence of *Bmi1+* cell clusters compared to younger animals. This appears to indicate that tissue renewal from the *Bmi1+* progenitor cells had slowed down. Another explanation could be that at 24 weeks the central cornea is more dependent on limbal input for tissue homeostasis. However, proliferative cells were present in the central cornea at 24 weeks, suggestive of regular cell divisions in the basal layer of the central cornea. Besides the central corneal cells, the LSCs seem to become more quiescent with age as well [5,9,36].

We challenged the capacity of the *Bmi1+* cells to renew the epithelium by inflicting an abrasion injury to the ocular surface. Majo et al., showed that large areas of corneal epithelium can heal without limbal input [20], and this is supported by evidence from LSC deficiency patients, who can maintain clear islets on the central cornea over a very long follow-up period [37]. On the other hand, upon chemical burn injury in mice, the LSCs are activated, but the extent of limbal input varies [3,6]. These results suggest that both central and limbal epithelial cells are responsive to ocular surface injury, possibly exerting different roles in the process of wound healing. After scraping the epithelium, the cornea healed fully within 72 hours, as reported earlier [38], but we could not detect a change in the *Bmi1+* cell progeny patterning nor the amount or distribution of the *Ki67+* cells. Instead, we saw that the epithelium was thin 18 hours after injury, which corresponds to the active period of healing. We propose that cell migration and reorganization of the epithelial layers, instead of proliferation, is the mode of healing after scraping injury. Our observation is supported by evidence from corneal epithelial cell culture, where addition of mitomycin C to the culture did not affect wound closure, suggesting that healing is not dependent on cell proliferation [39]. Interestingly, a similar mechanism, based on cell motility instead of proliferation

leading to cellular intercalation and convergent extension, was shown to be responsible for the eyelid closure in embryonic mice [40]. Our results are comparable to the re-epithelialization of rat cornea, which is not dependent on cell proliferation but rather on cell rearrangements [41]. We anticipate that *in vivo* wound healing occurs in several phases, as described by Suzuki et al. [42]. First the basal and suprabasal layers move on top of the exposed basement membrane, and only after that stratification begins and leads to full repopulation of all the epithelial cell layers. However, genetic fate mapping confirms that outside the exposed region epithelial turnover continues uninterrupted. Indeed, our analysis of epithelial thickness in the peripheral cornea shows that the migrating cell population does not originate from there. Instead, we suggest that the immediate wound edge at abrasion (0 hour) holds the epithelial cells that become activated upon wound healing. Finally, our cell proliferation analysis rules out extensive LSC activity after epithelial scraping and supports epithelial reorganization as the main resource for wound healing.

Collectively, our results reflect *Bmi1* expression in progenitor cells in the murine central cornea epithelium. *Bmi1* encodes a major component of the polycomb group complex 1 that functions in transcriptional control and chromatin remodeling [43–45]. Because of its large expression domain, *Bmi1* could play a role in progenitor behavior as opposed to stem cell self-renewal in the murine cornea epithelium. We believe that a further analysis of *Bmi1+* and negative cells can open up avenues to study the dynamic process of epithelial renewal in the cornea. It appears that corneal cells maintain an intricate hierarchy between different progenitor populations, and these populations function in separate but important processes.

Conclusions

Our experiments support the existence of central corneal progenitor cells and reveal that these progenitors maintain the corneal epithelium for a significant and limited time period, 4–8 weeks in young mice. *Bmi1* is expressed in these progenitor cells. Our analysis suggests as well that the cornea of a young mouse contains immature cells that will locate to the limbus by the end of corneal maturation. Epithelial scraping wounds showed that the *Bmi1+* cells maintain central turnover rate at a regular pace in wounded corneas and that wound healing occurs via epithelial cell reorganization rather than proliferation.

Supplementary Material

Refer to Web version on PubMed Central for supplementary material.

Acknowledgments

We would like to thank Kaisa Ikkala for her invaluable technical support and Kim Jensen for insightful feedback and comments during the project. We would also like to thank Danielle Dhouailly for her assistance. This research was supported by the Academy of Finland, the Jane and Aatos Erkko Foundation, NIDCR R35-DE026602 and the Doctoral School of Health, Integrative Life Science program, University of Helsinki.

References

1. Schermer A, Galvin S, Sun TT. Differentiation-related expression of a major 64K corneal keratin in vivo and in culture suggests limbal location of corneal epithelial stem cells. J Cell Biol. 1986; 103:49–62. [PubMed: 2424919]

2. Cotsarelis G, Cheng S-Z, Dong G, et al. Existence of slow-cycling limbal epithelial basal cells that can be preferentially stimulated to proliferate: Implications on epithelial stem cells. Cell. 1989; 57:201–209. [PubMed: 2702690]

3. Lehrer MS, Sun TT, Lavker RM. Strategies of epithelial repair: modulation of stem cell and transit amplifying cell proliferation. J Cell Sci. 1998; 111

4. Collinson JM, Morris L, Reid AI, et al. Clonal analysis of patterns of growth, stem cell activity, and cell movement during the development and maintenance of the murine corneal epithelium. Dev Dyn. 2002; 224:432–440. [PubMed: 12203735]

5. Dorà NJ, Hill RE, Collinson JM, et al. Lineage tracing in the adult mouse corneal epithelium supports the limbal epithelial stem cell hypothesis with intermittent periods of stem cell quiescence. Stem Cell Res. 2015; 15:665–677. [PubMed: 26554513]

6. Amitai-Lange A, Altshuler A, Bubley J, et al. Lineage Tracing of Stem and Progenitor Cells of the Murine Corneal Epithelium. Stem Cells. 2015; 33:230–239. [PubMed: 25187087]

7. Di Girolamo N, Bobba S, Raviraj V, et al. Tracing the Fate of Limbal Epithelial Progenitor Cells in the Murine Cornea. Stem Cells. 2015; 33:157–169. [PubMed: 24966117]

8. Pan YA, Freundlich T, Weissman TA, et al. Zebrabow: multispectral cell labeling for cell tracing and lineage analysis in zebrafish. Development. 2013; 140

9. Richardson A, Lobo EP, Delic NC, et al. Keratin-14-Positive Precursor Cells Spawn a Population of Migratory Corneal Epithelia that Maintain Tissue Mass throughout Life. Stem Cell Reports. 2017; 9:1081–1096. [PubMed: 28943255]

10. Zieske JD. Corneal development associated with eyelid opening. Int J Dev Biol. 2004; 48:903–911. [PubMed: 15558481]

11. Pajoohesh-Ganji A, Ghosh SP, Stepp MA. Regional distribution of a9b1 integrin within the limbus of the mouse ocular surface. Dev Dyn. 2004; 230:518–528. [PubMed: 15188436]

12. Eghtedari Y, Richardson A, Mai K, et al. Keratin 14 Expression in Epithelial Progenitor Cells of the Developing Human Cornea. Stem Cells Dev. 2016; 25:699–711. [PubMed: 26956898]

13. Tanifuji-Terai N, Terai K, Hayashi Y, et al. Expression of keratin 12 and maturation of corneal epithelium during development and postnatal growth. Investig Ophthalmol Vis Sci. 2006; 47:545–551. [PubMed: 16431949]

14. Park I, Qian D, Kiel M, et al. Bmi-1 is required for maintenance of adult self-renewing haematopoietic stem cells. Nature. 2003; 423:302–305. [PubMed: 12714971]

15. Iwama A, Oguro H, Negishi M, et al. Enhanced Self-Renewal of Hematopoietic Stem Cells Mediated by the Polycomb Gene Product Bmi-1. Immunity. 2004; 21:843–851. [PubMed: 15589172]

16. Molofsky A V, Pardal R, Iwashita T, et al. Bmi-1 dependence distinguishes neural stem cell self-renewal from progenitor proliferation. Nature. 2003; 425:962–967. [PubMed: 14574365]

17. Biehs B, Hu JK-H, Strauli NB, et al. BMI1 represses Ink4a/Arf and Hox genes to regulate stem cells in the rodent incisor. Nat Cell Biol. 2013; 15:846–852. [PubMed: 23728424]

18. Barbaro V, Testa A, Di Iorio E, et al. C/EBPδ regulates cell cycle and self-renewal of human limbal stem cells. J Cell Biol. 2007; 177:1037–1049. [PubMed: 17562792]

19. Levis HJ, Daniels JT. Recreating the Human Limbal Epithelial Stem Cell Niche with Bioengineered Limbal Crypts. Curr Eye Res. 2016; 41:1153–1160. [PubMed: 26727236]

20. Majo F, Rochat A, Nicolas M, et al. Oligopotent stem cells are distributed throughout the mammalian ocular surface. Nature. 2008; 456:250–254. [PubMed: 18830243]

21. Van Der Lugt NMT, Domen J, Linders K, et al. Posterior transformation, neurological abnormalities, and severe hematopoietic defects in mice with a targeted deletion of the bmi-1 proto-oncogene. Genes Dev. 1994; 8:757–769. [PubMed: 7926765]

22. López-Arribillaga E, Rodilla V, Pellegrinet L, et al. Bmi1 regulates murine intestinal stem cell proliferation and self-renewal downstream of Notch. Development. 2014; 142:41–50. [PubMed: 25480918]

23. Liu J, Cao L, Chen J, et al. Bmi1 regulates mitochondrial function and the DNA damage response pathway. Nature. 2009; 459

24. Sangiorgi E, Capecchi MR. Bmi1 is expressed in vivo in intestinal stem cells. Nat Genet. 2008; 40:915–920. [PubMed: 18536716]
25. Soriano P. Generalized lacZ expression with the ROSA26 Cre reporter strain. Nat Genet. 1999; 21:70–71. [PubMed: 9916792]
26. Pispa J, Pummila M, Barker PA, et al. Edar and Troy signalling pathways act redundantly to regulate initiation of hair follicle development. Hum Mol Genet. 2008; 17:3380–3391. [PubMed: 18689798]
27. Echevarria TJ, Di Girolamo N. Tissue-Regenerating, Vision-Restoring Corneal Epithelial Stem Cells. Stem Cell Rev Reports. 2010; 7:256–268.
28. Lauweryns B, Van den Oord JJ, Missotten L. The transitional zone between limbus and peripheral cornea: An immunohistochemical study. Investig Ophthalmol Vis Sci. 1993; 34:1991–1999. [PubMed: 8387976]
29. Kasper M, Moll R, Stosiek P, et al. Patterns of cytokeratin and vimentin expression in the human eye. Histochemistry. 1988; 89:369–377. [PubMed: 2457569]
30. Yoshida S, Shimmura S, Kawakita T, et al. Cytokeratin 15 Can Be Used to Identify the Limbal Phenotype in Normal and Diseased Ocular Surfaces. Investig Opthalmology Vis Sci. 2006; 47:4780.
31. Ramirez-Miranda A, Nakatsu MN, Zarei-Ghanavati S, et al. Keratin 13 is a more specific marker of conjunctival epithelium than keratin 19. Mol Vis. 2011; 17:1652–1661. [PubMed: 21738394]
32. Davies SB, Chui J, Madigan MC, et al. Stem Cell Activity in the Developing Human Cornea. Stem Cells. 2009; 27:2781–2792. [PubMed: 19711455]
33. Dobie K, Mehtali M, McClenaghan M, et al. Variegated gene expression in mice. Trends Genet. 1997; 13:127–130. [PubMed: 9097721]
34. Douvaras P, Webb S, Whitaker DA, et al. Rare corneal clones in mice suggest an age-related decrease of stem cell activity and support the limbal epithelial stem cell hypothesis. Stem Cell Res. 2012; 8:109–119. [PubMed: 22099025]
35. Nagasaki T, Zhao J. Centripetal Movement of Corneal Epithelial Cells in the Normal Adult Mouse. Investig Opthalmology Vis Sci. 2003; 44:558.
36. Mort RL, Ramaesh T, Kleinjan DA, et al. Mosaic analysis of stem cell function and wound healing in the mouse corneal epithelium. BMC Dev Biol. 2009; 9:4. [PubMed: 19128502]
37. Dua HS, Miri A, Alomar T, et al. The Role of Limbal Stem Cells in Corneal Epithelial Maintenance. Ophthalmology. 2009; 116:856–863. [PubMed: 19410942]
38. Sartaj R, Chee R, Yang J, et al. LIM Homeobox Domain 2 Is Required for Corneal Epithelial Homeostasis. Stem Cells. 2016; 34:493–503. [PubMed: 26661907]
39. Kaplan N, Fatima A, Peng H, et al. EphA2/Ephrin-A1 Signaling Complexes Restrict Corneal Epithelial Cell Migration. Investig Opthalmology Vis Sci. 2012; 53:936.
40. Heller E, Kumar KV, Grill SW, et al. Forces generated by cell intercalation tow epidermal sheets in mammalian tissue morphogenesis. Dev Cell. 2014; 28:617–632. [PubMed: 24697897]
41. Chung EH, Hutcheon AE, Joyce NC, et al. Synchronization of the G1/S transition in response to corneal debridement. Invest Ophthalmol Vis Sci. 1999; 40:1952–1958. [PubMed: 10440248]
42. Suzuki K. Cell–matrix and cell–cell interactions during corneal epithelial wound healing. Prog Retin Eye Res. 2003; 22:113–133. [PubMed: 12604055]
43. van Lohuizen M, Jacobs JJL, Kieboom K, et al. The oncogene and Polycomb-group gene bmi-1 regulates cell proliferation and senescence through the ink4a locus. Nature. 1999; 397:164–168. [PubMed: 9923679]
44. Gould A. Functions of mammalian Polycomb group and trithorax group related genes. Curr Opin Genet Dev. 1997; 7:488–494. [PubMed: 9309179]
45. Paro R. Propagating memory of transcriptional states. Trends Genet. 1995; 11:295–297. [PubMed: 8585123]

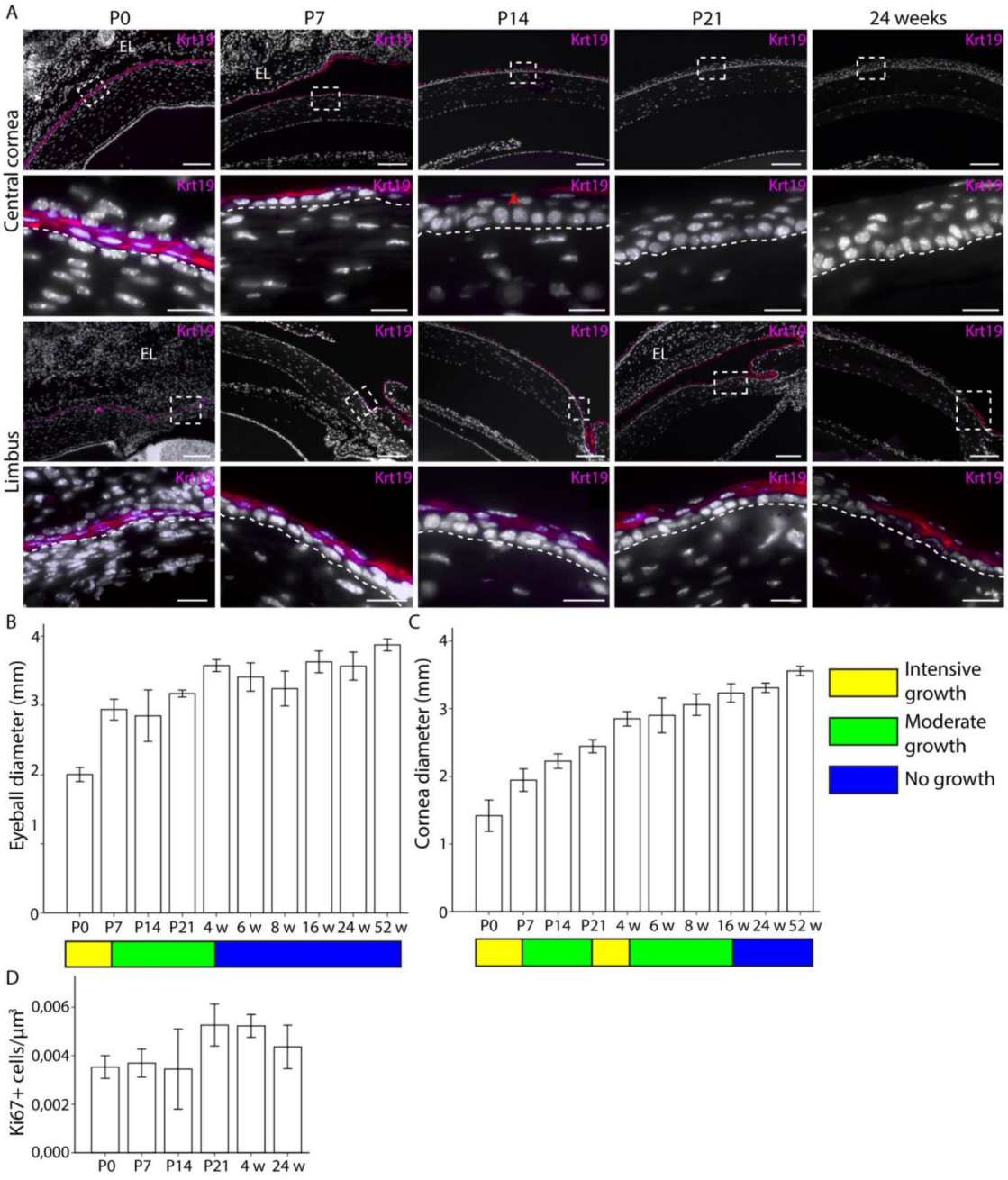

Figure 1.

Krt19 expression pattern correlates with cornea growth and maturation. *Krt19* expressing cells are marked with magenta. **(A)**: At P0, all corneal epithelial cells were *Krt19+*. Boxes indicate the location of insets. At P7, the expression domain excluded the basal cells in the central and limbal cornea. The border between epithelium and stroma is marked with a dashed line. By P14, the central corneal epithelial cells were almost all *Krt19*-negative (arrowhead), but the limbal epithelial cells were *Krt19+*. At P21, we could not detect *Krt19* expression in the central cornea anymore, in contrast to noticeable expression in the limbus. After that the expression pattern remained constant; at 24 weeks of age the limbal epithelial

cells were *Krt19+*. However, signal from the central and peripheral cornea was completely lost. **(B-C)**: Growth rate is indicated with a color pattern: yellow for intensive growth, green for moderate growth and blue for no more growth. **(B)**: Eyeball diameter increased quickly from P0 until P7 ($p=0.000$), then with moderate pace from P7 until 4 weeks ($p=0.000$); after that growth ceased ($p \geq 0.474$). **(C)**: Cornea diameter increased stepwise between P0 and P7 ($P=0.000$) as well as between P21 and 4 weeks ($p=0.005$), with periods of moderate growth ($p=0.000$) after each quick growth phase. Cornea diameter did not increase anymore after 16 weeks of age ($p \geq 0.193$). **(D)**: The amount proliferating, *Ki67+* cells were steadily maintained in an appropriate level at each age ($p \geq 0.125$). Errors bars indicate 2 ± standard error. Hoechst for nuclear staining (white). Eyelid (EL). Scale bars are 100 μm, 20 μm for insets.

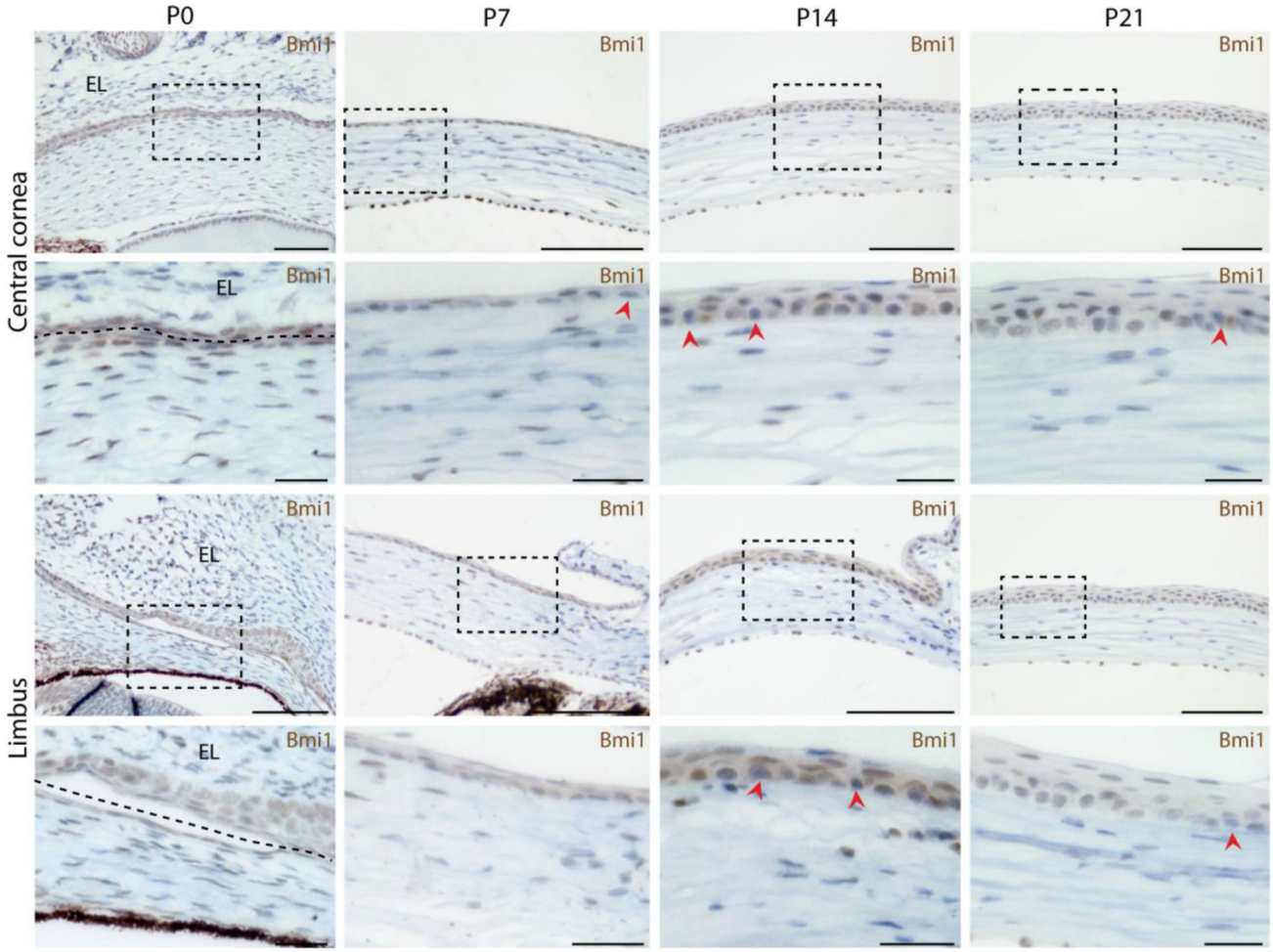

Figure 2.

Bmi1 expression is steady during cornea maturation. BMI1 immunostaining in brown. *Bmi1* is expressed throughout both epithelial layers before epithelial stratification begins (boxes show the location of insets). The border between corneal epithelium and inner eyelid is marked with a dashed line. P14 marks the beginning of eyelid opening and epithelial stratification. *Bmi1* is mostly expressed in the basal epithelium, but visible also in the suprabasal epithelium. All layers contain some *Bmi1*-negative cells (arrowheads). At P21 *Bmi1* becomes more confined to the basal epithelium, however, rare *Bmi1*-negative cells remain as well as some *Bmi1+* in the suprabasal layer. Hematoxylin for nuclear staining (blue). Scale bars are 100 μm, 25 μm for the insets.

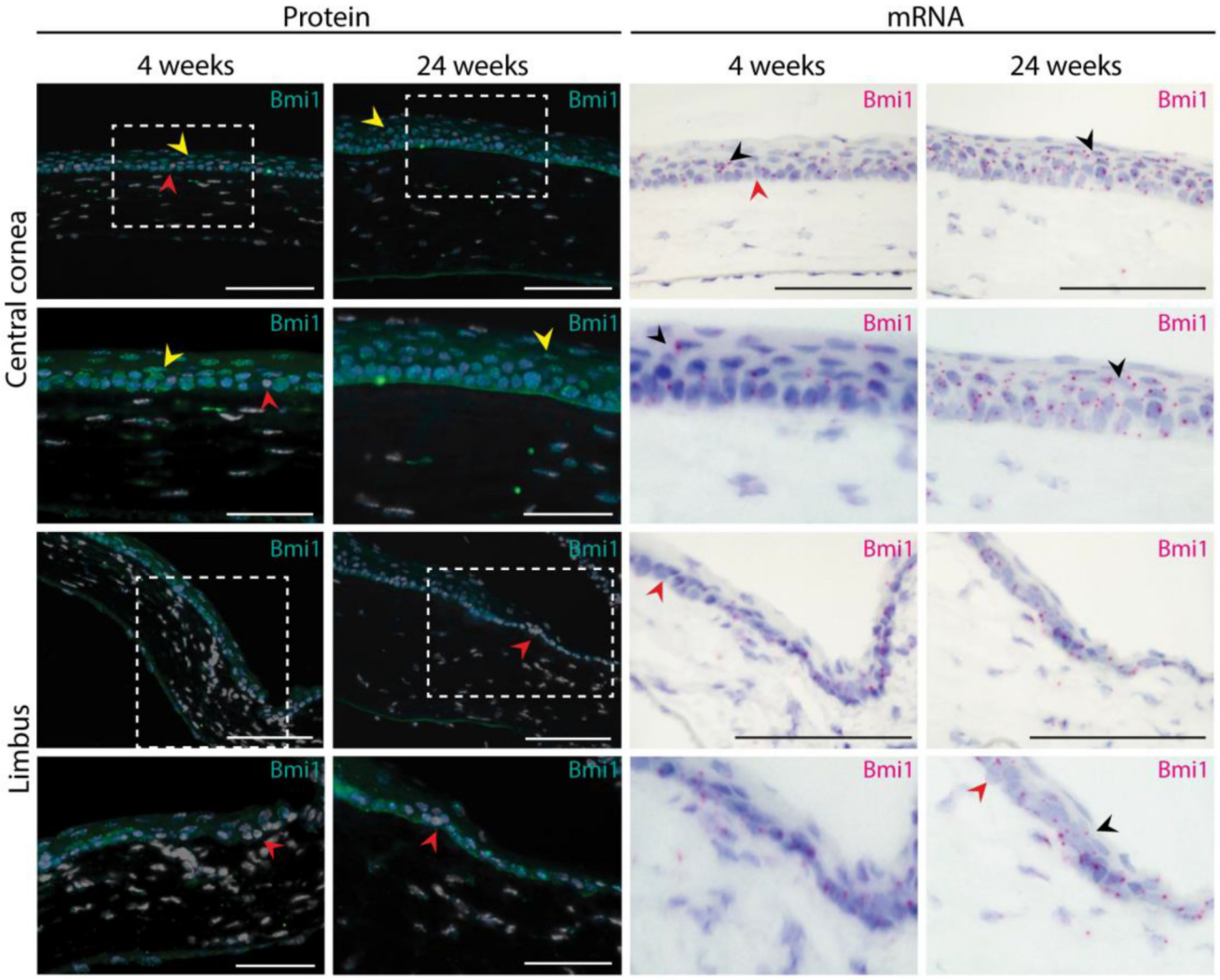

Figure 3.

Bmi1 expression pattern remains unchanged after cornea maturation. We assayed both BMI1 protein (in turquoise) and *Bmi1* RNA (in magenta). Young (4 weeks old) and adult mice (24 weeks old) displayed the same expression pattern. Most of the epithelial basal cell layer of the cornea was composed of *Bmi1+* cells. In both stages, we discovered few *Bmi1*-negative cells in the basal layer (red arrowhead). Some suprabasal cells expressed *Bmi1* in the adult cornea (yellow or black arrowhead). Hoechst for nuclear staining (white) and hematoxylin for nuclear staining (blue). Scale bars are 100 μm, 50 μm for the insets.

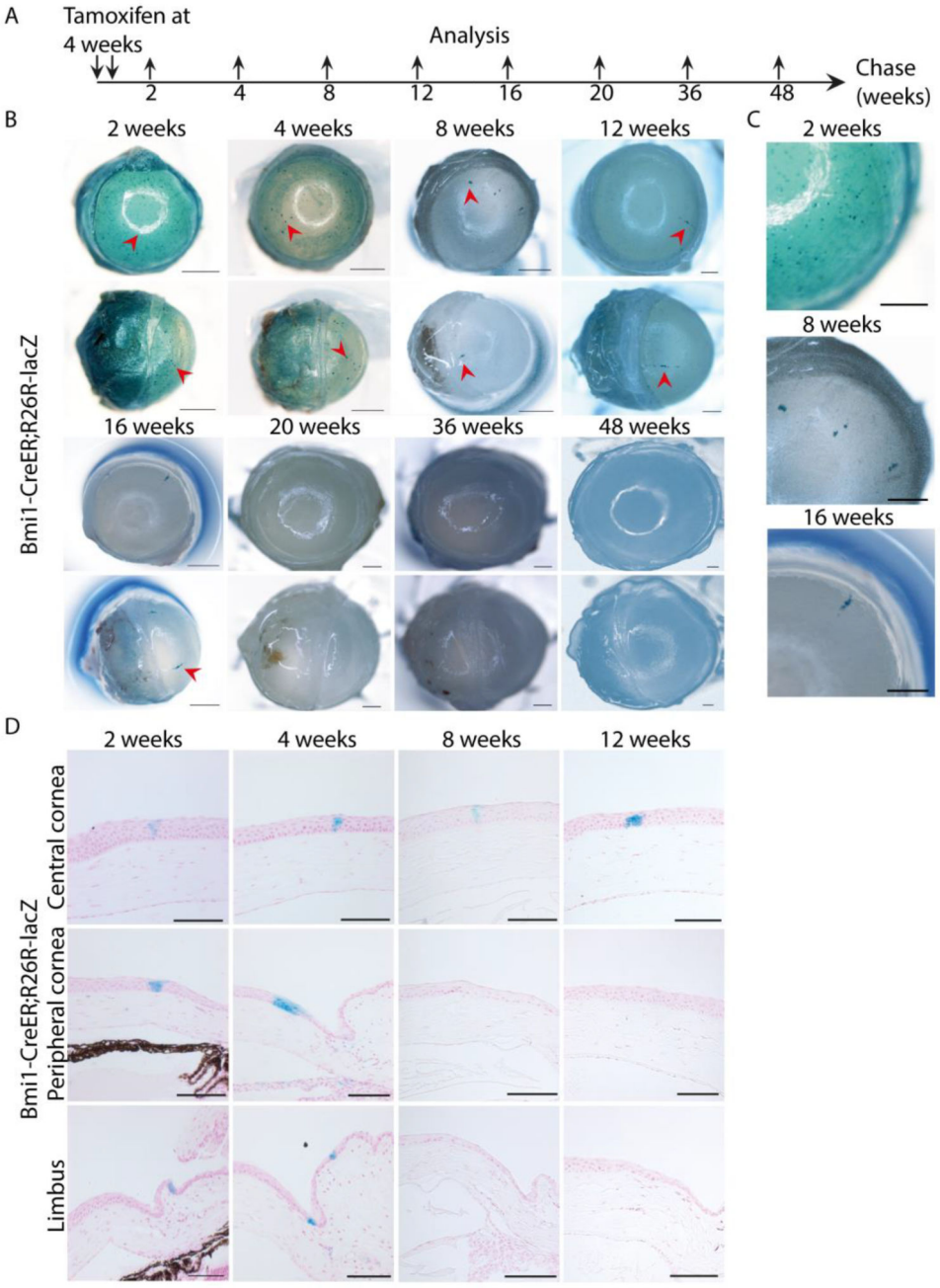

Figure 4.

Genetic fate mapping of *Bmi1+* cells reveals progenitor-like dynamics. **(A)**: Schematic drawing of the genetic fate mapping experiment. The recombinase was induced at 4 weeks of age and eyeballs were regularly collected after 2 to 48 weeks of chase. **(B)**: *Bmi1+* cells and their progeny are marked in blue due to *LacZ* expression. The bright ring on top of the central cornea is a technical artefact from the camera. For each time point, we sacrificed 3 littermates and chose a representative image to showcase. After 2 and 4 weeks post-induction, blue cell clusters emerged in the central, peripheral and limbal cornea (arrowheads). Between 8 and 16 weeks of chase, these clusters gradually disappeared,

leaving few stripes visible (arrowheads). We did not note any progeny from 20 weeks onwards. **(C)**: Insets of cornea after 2, 8 and 16 weeks of chase. **(D)**: The histological sections confirmed that *Bmi1+* cells and their progeny formed columnar clones within the epithelium in the central, peripheral and limbal cornea after short chases. Nuclear FAST red for nuclear staining (red). Scale bars are 1 mm **(B-C)** and 100 μm **(D)**.

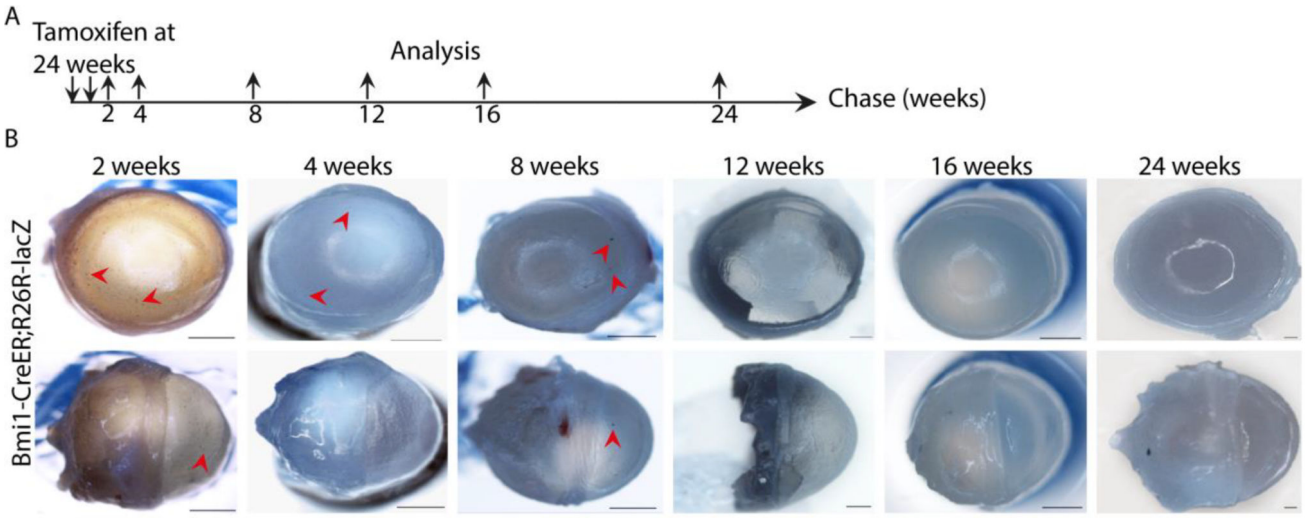

Figure 5.

Genetic fate mapping of *Bmi1+* cells shows short-lived clones in fully mature mice. **(A)**: Schematic drawing of the genetic fate mapping experiment. The recombinase was induced at 24 weeks of age and eyeballs were regularly collected after 2 to 24 weeks of chase. **(B)**: We observed *Bmi1+*, rare clusters in the cornea after 2, 4 and 8 weeks of chase (arrowheads). After 12 weeks of chase, *Bmi1+* cells did not produce new progeny. Scale bars are 1 mm.

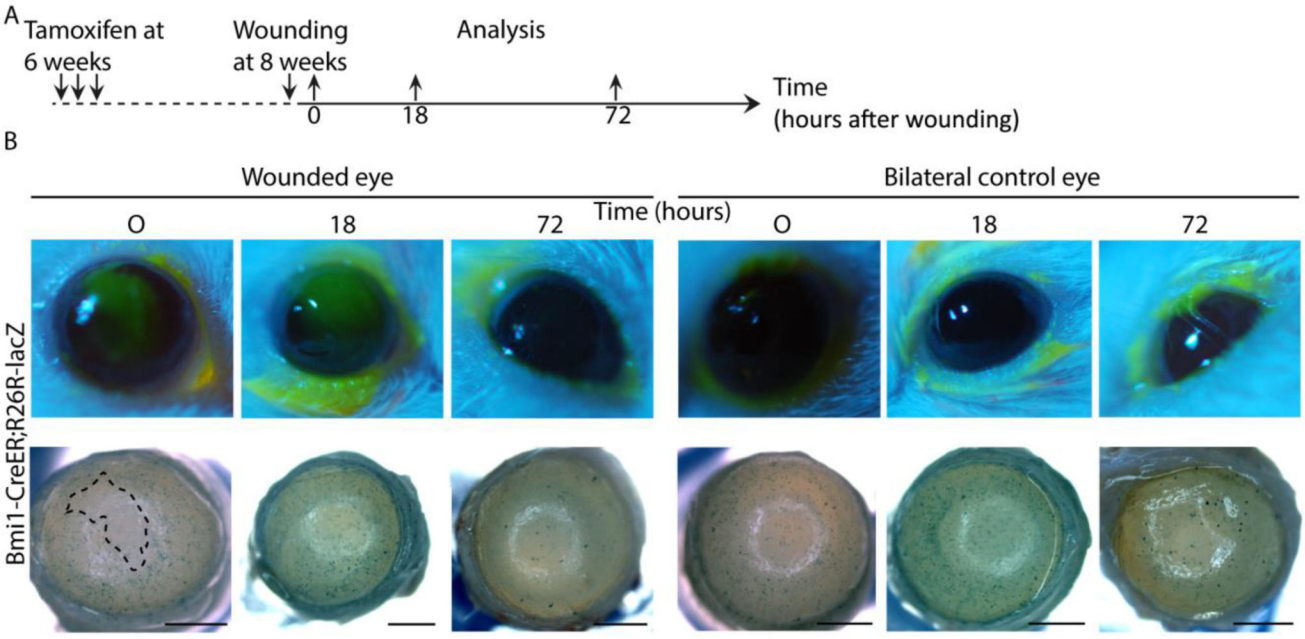

Figure 6.

Corneal wounding reveals that *Bmi1+* cells are not proliferative upon injury. **(A)**: *LacZ* expression was induced at 6 weeks in $Bmi1^{CreERT/wt}$;$R26R^{LacZ/wt}$ mice, followed by a scraping wound 2 weeks later on one eye/animal. We collected both eyes immediately after wounding, 18 hours or 72 hours after. For each time point, we sacrificed 3 littermates and chose a representative image to showcase. **(B)**: Fluorescein staining in green shows the wounded region and an area devoid of cells, e.g. the wounded area, is marked with a dashed line in the lower panel. The wound is still clear after 18 hours, but fate mapping shows a normal, patchy pattern outside the wounded region. By 72 hours after wounding, the cornea is fully healed and central renewal pattern follows a regular pattern. Right panels show the bilateral, unwounded control eye at each time point. Scale bar is 1 mm.

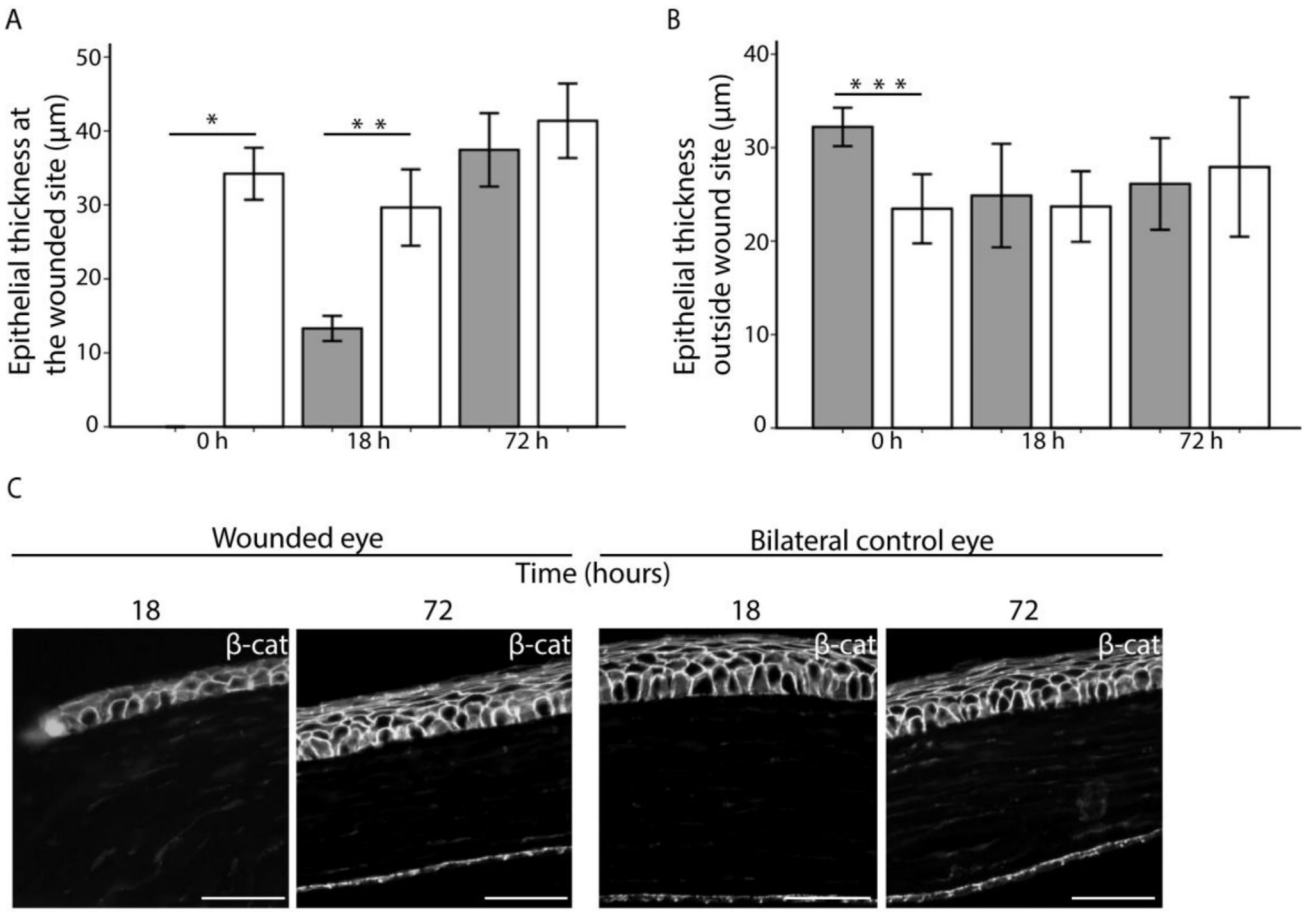

Figure 7.

Epithelial thickness changes during wound healing. **(A)**: Estimation of epithelial thickness 0, 18 and 72 hours post injury in the center of the cornea (grey bars). Control samples (white bars) represent the thickness of the epithelium in the bilateral, unwounded eyes in a similar location. The epithelium was significantly thinner in the cornea 0 hours (p=0.000) and 18 hours (p=0.001) after injury. **(B)**: Thickness of the epithelium in peripheral cornea after 0, 18 and 72 hours post injury. The control epithelium was significantly thinner at 0 hours (p=0.002), which might reflect retraction of the epithelium due to loosened mechanimal forces just after abrasion. At other time points, epithelium was not thinner in the abrased cornea compared to the control. **(C)**: The re-epithelializing zone 18 hours after injury consists of only two epithelial cell layers. Epithelium has recovered at 72 hours. Unwounded control eyes. β-catenin (in white) shows cell borders. Scale bar is 50 µm. Error bars indicate 2 ± standard error.